Received 16 December 2024
Revised 20 May 2025
Accepted 20 May 2025

An effective interface formulation for electromagnetic shielding using the A-formulation in 3D

Markus Schöbinger, Michael Leumüller and Karl Hollaus
Institute of Analysis and Scientific Computing, Technische Universitat Wien, Wien, Austria

Abstract

Purpose – The purpose of this paper is to present an effective material approach to simulate electromagnetic shields using the A-Formulation in a fully 3D setting with nonlinear materials in the frequency domain. It allows to treat the shield as an interface in the finite element mesh so that only the magnetic vector potential in the surrounding air has to be considered for the solution.

Design/methodology/approach – The jump of the tangential components of the potential across the interface is controlled by an effective material parameter based on a suitable cell problem. This parameter can be efficiently interpolated from a precomputed look-up table.

Findings – The method is able to consider curved shields and holes. A numerical example shows an excellent agreement of the presented method compared to a reference solution both in a global and a local sense.

Originality/value – A novel effective material approach based on numerical solutions of a suitable nonlinear cell problem is presented.

Keywords Electromagnetic shielding, Thin shell model, Effective material, Eddy currents, Electromagnetic fields, Magnetic shielding, Homogenization method

Paper type Research paper

1. Introduction

To comply with electromagnetic compatibility and to reduce the exposure of human beings, shielding is an essential component in a wide range of applications. To reduce both the cost and the weight, it is of interest to use shields which are as thin as possible while still fulfilling the given requirements. This poses significant challenges for the simulation.

Because the thickness of the sheets used for shielding is very small compared to the overall dimensions of the geometry, the finite element mesh needs to include either an unfeasible amount of elements, or very anisotropic elements in the vicinity of the shield. Furthermore, due to the material properties of the shield, the fields can vary strongly across its thickness, requiring a fine discretization in the conducting region. These two issues lead to badly conditioned finite element systems and a high number of degrees of freedom (Geuzaine *et al.*, 2000).

COMPEL - The international journal for computation and mathematics in electrical and electronic engineering
Vol. 44 No. 5, 2025
pp. 756-768
Emerald Publishing Limited
0332-1649
DOI 10.1108/COMPEL-12-2024-0519

This research was funded in whole or in part by the Austrian Science Fund (FWF) [10.55776/P36395]. For open access purposes, the author has applied a CC BY public copyright license to any author accepted manuscript version arising from this submission.

The classic approach is to treat the shields using thin shell models (Rodger *et al.*, 1988; Mayergoyz and Bedrosian, 1995). These replace the thin sheets with an interface of zero thickness and derive a suitable impedance type boundary conditions based on an approximate behavior of the solution inside the shield.

For shields with a low enough thickness, it suffices to use a strip approximation using a linear potential distribution (Krähenbühl and Muller, 1993; Igarashi *et al.*, 1998; Hong *et al.*, 2007; Liang *et al.*, 2017). Similarly, Koch *et al.* (2009), presents a shell element method for a metallic beam tube under the assumption that the thickness is small compared to the skin depth of the eddy currents. This has been refined in Taha *et al.* (2023) using a formulation based on the Darwin model.

A common approach is to collapse the shield by replacing it locally by a one-dimensional cell problem (Bottauscio *et al.*, 2006; Rasilo *et al.*, 2020; Biro *et al.*, 1997; Fujita and Igarashi, 2019). For linear materials, an analytic solution of this cell problem is available, which allows for a direct derivation of the interface condition.

Because classic impedance conditions on interfaces only hold for linear materials, the nonlinear case requires an appropriate correction, as has been carried out for example in Del Vecchio and Ahuja, (2013). A method to obtain a suitable boundary condition for the case of a piecewise linear BH-curve is presented in Ortega *et al.* (2024).

When considering the nonlinear cell problem where no analytic solution exists, one can use a local expansion using suitable basis functions to obtain an approximation of the cell solution, as has been done for example in de Sousa Alves *et al.* (2021). This increases the accuracy at the cost of additional degrees of freedom.

This work is based on the classic linear formulation using an analytic solution in the cell problem and extends it to the nonlinear case using an effective material approach similar to Schöbinger *et al.* (2021). The main idea is to treat the material-dependent constants inside the analytic solution as parameters which are fitted such that this modified solution achieves the correct reactive power. To prevent the need for repeated calculations of numerical solutions on the cell problem, the effective material parameters are interpolated from a precomputed look-up table.

The performance of the presented method is demonstrated by a numerical example using a curved shield over a current loop. Both the global properties inside the shield and the local field distributions are compared to a reference solution and show very satisfying results.

2. Problem formulation

The main application is an electromagnetic shield over a source, which redirects the magnetic flux along its surface while inducing eddy currents, and thereby shields the area behind it, see Figure 1.

As a mathematical description we consider the eddy current problem in the frequency domain, which is given by:

$$\begin{aligned} \mathrm{curl}\boldsymbol{H} &= \boldsymbol{J}, \\ \mathrm{curl}\boldsymbol{E} &= -i\omega\boldsymbol{B}, \\ \mathrm{div}\boldsymbol{B} &= 0, \\ \boldsymbol{J} &= \sigma\boldsymbol{E}, \\ \boldsymbol{B} &= \mu\boldsymbol{H}, \end{aligned} \tag{1}$$

where $\boldsymbol{E}$ is the electric field, $\boldsymbol{J}$ the current density, $\boldsymbol{H}$ the magnetic field, $\boldsymbol{B}$ the magnetic flux density, μ the (possibly nonlinear) magnetic permeability, σ the electric conductivity, $\omega = 2\pi f$ the angular frequency with the frequency f, and i the imaginary unit.

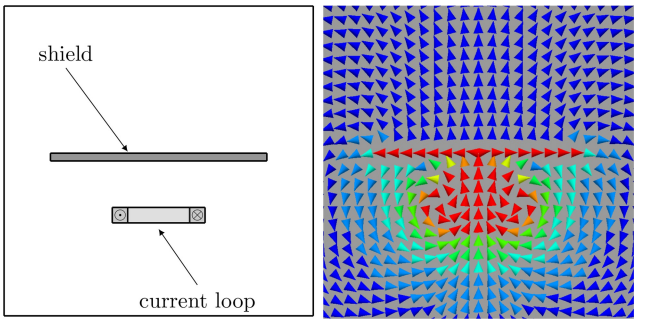

Figure 1. A shield above a current loop (left) redirects the magnetic flux (right)
Source: Authors' own work

By introducing the magnetic vector potential $\boldsymbol{A}$ with curl$\boldsymbol{A} = \boldsymbol{B}$ and $i\omega\boldsymbol{A} = \boldsymbol{E}$, the strong form of the eddy current problem is given as:

$$\text{curl}\nu\text{curl}\boldsymbol{A} + i\omega\sigma\boldsymbol{A} = \boldsymbol{J}_0, \tag{2}$$

where $\nu = \mu^{-1}$ is the magnetic reluctivity and $\boldsymbol{J}_0$ the given currents of the excitation.

Multiplication with a test function $\boldsymbol{v}$ and integration over the entire domain Ω yields the corresponding weak formulation: Find $\boldsymbol{A} \in H(\text{curl})$ so that:

$$\begin{aligned} &\int \nu\text{curl}\boldsymbol{A} \cdot \text{curl}\boldsymbol{v} + i\omega\sigma\boldsymbol{A} \cdot \boldsymbol{v}\, d\Omega \\ &= \int \boldsymbol{H}_{BS} \cdot \text{curl}\boldsymbol{v}\, d\Omega \end{aligned} \tag{3}$$

for all $\boldsymbol{v} \in H$ (curl) where $\boldsymbol{H}_{BS}$ denotes the Biot-Savart fields of the given currents, fulfilling curl$\boldsymbol{H}_{BS} = \boldsymbol{J}_0$.

3. The effective interface formulation

Let Ω_c denote the conducting domain, i.e. the shield, and $\Omega_0 = \Omega \setminus \Omega_c$ the surrounding air. The objective is to replace the shield with an interface Γ in the finite element mesh by decomposing the domain according to $\Omega_c = \Gamma \times \left[-\frac{d}{2}, \frac{d}{2}\right]$ where d is the thickness of the shield. The thickness is then neglected and the solutions on both sides of the interface are coupled on each point of Γ by a suitable one-dimensional cell problem.

3.1 A The cell problem

In this section the material is assumed to be linear. For a given point on Γ let $\boldsymbol{t}_1$,$\boldsymbol{t}_2$ be two orthogonal positively oriented tangential vectors of unit length and η the coordinate in normal direction. Because the normal currents are negligible compared to the tangential currents inside the shield, we use the approximation:

$$\begin{aligned} \boldsymbol{A} \approx \widetilde{\boldsymbol{A}} &= A_1(\eta)\boldsymbol{t}_1 + A_2(\eta)\boldsymbol{t}_2, \\ A_i &= \boldsymbol{A} \cdot \boldsymbol{t}_i \end{aligned} \tag{4}$$

for the solution inside the shield. Accordingly, the magnetic flux density is given as:

$$\widetilde{\boldsymbol{B}} = \mathrm{curl}\widetilde{\boldsymbol{A}} = -\frac{\partial}{\partial\eta}A_2(\eta)\boldsymbol{t}_1 + \frac{\partial}{\partial\eta}A_1(\eta)\boldsymbol{t}_2. \tag{5}$$

Let $\boldsymbol{A}^+$ and $\boldsymbol{A}^-$ denote the tangential components of the solution on the top and the bottom of the shield, respectively. The strong formulation for the 1D cell problem can then be written as

$$\begin{aligned} \mathrm{curl}\nu\mathrm{curl}\widetilde{\boldsymbol{A}} + i\omega\sigma\widetilde{\boldsymbol{A}} &= 0, \\ \widetilde{\boldsymbol{A}}\left(\pm\frac{d}{2}\right) &= \boldsymbol{A}^{\pm}, \end{aligned} \tag{6}$$

assuming that there are no given excitation currents inside the shield.

Because of the structure of $\widetilde{\boldsymbol{A}}$ given in (4) this can be further simplified to:

$$\begin{aligned} -\frac{\partial}{\partial\eta}\left(\nu\frac{\partial}{\partial\eta}A_i(\eta)\right) + i\omega\sigma A_i(\eta) &= 0, \\ A_i\left(\pm\frac{d}{2}\right) &= A_i^{\pm}, \end{aligned} \tag{7}$$

with $A_i^{\pm} = \boldsymbol{A}^{\pm}\cdot\boldsymbol{t}_j$. Note that the equations for the components would not decouple in the nonlinear case, because then $\nu = \nu(\|\widetilde{\boldsymbol{A}}\|)$.

The analytic solution of (7) is given by:

$$A_i(\eta) = c_{i1}e^{\gamma\eta} + c_{i2}e^{-\gamma\eta}, \tag{8}$$

where $\gamma = \sqrt{i\omega\sigma\nu^{-1}}$. The constants $c_{i,j}$ are given as:

$$\begin{aligned} c_{i1} &= \frac{A_i^+e^{\gamma\frac{d}{2}} - A_i^-e^{-\gamma\frac{d}{2}}}{e^{\gamma d} - e^{-\gamma d}}, \\ c_{i2} &= \frac{A_i^-e^{\gamma\frac{d}{2}} - A_i^+e^{-\gamma\frac{d}{2}}}{e^{\gamma d} - e^{-\gamma d}}. \end{aligned} \tag{9}$$

3.2 B The interface formulation

The main idea is to treat the shield separately in the weak formulation and use the solution of the cell problem in Ω_c for both the trial function and the test function to obtain an equation of the form:

$$\begin{aligned} &\int_{\Omega_0}\nu\mathrm{curl}\boldsymbol{A}\cdot\mathrm{curl}\boldsymbol{\nu}d\Omega + \int_{\Omega_c}\nu\mathrm{curl}\widetilde{\boldsymbol{A}}\cdot\mathrm{curl}\widetilde{\boldsymbol{\nu}} + i\omega\sigma\widetilde{\boldsymbol{A}}\cdot\widetilde{\boldsymbol{\nu}}d\Omega \\ &= \int_{\Omega_0}\boldsymbol{H}_{BS}\cdot\mathrm{curl}\boldsymbol{\nu}d\Omega + \int_{\Omega_c}\boldsymbol{H}_{BS}\cdot\mathrm{curl}\widetilde{\boldsymbol{\nu}}d\Omega. \end{aligned} \tag{10}$$

This leads to an immediate reduction in the number of unknowns, because $\widetilde{\boldsymbol{A}}$ is fully determined by the tangential components of $\boldsymbol{A}$ on the boundary of Ω_c, i.e. it suffices to solve for an unknown function $\boldsymbol{A}\in H(\mathrm{curl},\Omega_0)$.

To replace Ω_c with the interface Γ, the relevant domain integrals are decomposed according to

$$\int_{\Omega_c} d\Omega = \int_{\Gamma_c}\int_{-\frac{d}{2}}^{\frac{d}{2}} d\eta d\Gamma. \tag{11}$$

Because $\widetilde{\boldsymbol{A}}(\eta)$ is explicitly given by (8) and (9), it is possible to carry out the integration with respect to η analytically. Note that the constants given in (9), and therefore also the solution of the cell problem, depend linearly on the solution in Ω_0. Therefore the formulation (10) still has the structure of a bilinear form on the left hand side and a linear form on the right hand side.

The final weak formulation is given as: Find $\boldsymbol{A} \in H(\mathrm{curl},\Omega_0)$ so that:

$$\begin{aligned}
&\int_{\Omega_0} \nu \mathrm{curl}\boldsymbol{A} \cdot \mathrm{curl} v,\, d\Omega \\
&+ \int_{\Gamma} S_0 \begin{pmatrix} A_1^+ & A_1^- \end{pmatrix} \begin{pmatrix} S_{11} & S_{12} \\ S_{21} & S_{22} \end{pmatrix} \begin{pmatrix} v_1^+ \\ v_1^- \end{pmatrix} d\Gamma \\
&+ \int_{\Gamma} S_0 \begin{pmatrix} A_2^+ & A_2^- \end{pmatrix} \begin{pmatrix} S_{11} & S_{12} \\ S_{21} & S_{22} \end{pmatrix} \begin{pmatrix} v_2^+ \\ v_2^- \end{pmatrix} d\Gamma \\
&+ \int_{\Gamma} M_0 \begin{pmatrix} A_1^+ & A_1^- \end{pmatrix} \begin{pmatrix} M_{11} & M_{12} \\ M_{21} & M_{22} \end{pmatrix} \begin{pmatrix} v_1^+ \\ v_1^- \end{pmatrix} d\Gamma \\
&+ \int_{\Gamma} M_0 \begin{pmatrix} A_2^+ & A_2^- \end{pmatrix} \begin{pmatrix} M_{11} & M_{12} \\ M_{21} & M_{22} \end{pmatrix} \begin{pmatrix} v_2^+ \\ v_2^- \end{pmatrix} d\Gamma \\
&= \int_{\Omega_0} \boldsymbol{H}_{BS} \cdot \mathrm{curl} v d\Omega \\
&+ \int_{\Gamma} \boldsymbol{H}_{BS} \cdot \boldsymbol{t}_2 v_1^- - \boldsymbol{H}_{BS} \cdot \boldsymbol{t}_2 v_1^+ d\Gamma \\
&+ \int_{\Gamma} \boldsymbol{H}_{BS} \cdot \boldsymbol{t}_1 v_2^+ - \boldsymbol{H}_{BS} \cdot \boldsymbol{t}_1 v_2^- d\Gamma
\end{aligned} \tag{12}$$

for all $\boldsymbol{v}. \in H(\mathrm{curl}\ \Omega_0)$, where the stiffness coefficients are given by:

$$\begin{aligned}
S_0 &= \frac{\gamma\nu}{2\left(e^{\gamma d} - e^{-\gamma d}\right)^2}, \\
S_{11} &= S_{22} = e^{2\gamma d} + 4\gamma d - e^{-2\gamma d}, \\
S_{12} &= S_{21} = 2\left(e^{-\gamma d} - e^{\gamma d}\right) - 2\gamma d\left(e^{\gamma d} + e^{-\gamma d}\right),
\end{aligned} \tag{13}$$

the mass coefficients by:

$$
\begin{aligned}
M_0 &= \frac{i\omega\sigma}{2\gamma\left(e^{\gamma d} - e^{-\gamma d}\right)^2},\\
M_{11} &= M_{22} = e^{2\gamma d} - 4\gamma d - e^{-2\gamma d},\\
M_{12} &= M_{21} = 2\left(e^{-\gamma d} - e^{\gamma d}\right) + 2\gamma d\left(e^{\gamma d} + e^{-\gamma d}\right),
\end{aligned}
\tag{14}
$$

and the subscripts and superscripts denote the tangential component and whether the values are taken from the top or the bottom, like it has been defined for the cell problem. Note that the solution $\boldsymbol{A}$ is not tangentially continous across Γ, so the used finite element space needs to allow for a jump.

In a postprocessing step, the total reactive power Q given as:

$$
Q = \frac{\omega}{2}\int_{\Omega_c} \nu \boldsymbol{B}\cdot\boldsymbol{B}^* d\Omega \tag{15}
$$

and the total losses P given as:

$$
P = \frac{1}{2}\int_{\Omega_c} \sigma \boldsymbol{E}\cdot\boldsymbol{E}^* d\Omega \tag{16}
$$

can be similarly evaluated by substituting the analytic cell solution at every point on Γ and carrying out integration with respect to η.

Let c_{ij} be defined as in (9) as functions of the calculated finite element solution $\boldsymbol{A}$. The total reactive power can be obtained by:

$$
\begin{aligned}
Q = &\int_\Gamma Q_0 \begin{pmatrix} c_{11} & c_{12}\end{pmatrix} \begin{pmatrix} Q_{11} & Q_{12}\\ Q_{21} & Q_{22}\end{pmatrix} \begin{pmatrix} c_{11}^*\\ c_{12}^*\end{pmatrix} d\Gamma\\
&+ \int_\Gamma Q_0 \begin{pmatrix} c_{21} & c_{22}\end{pmatrix} \begin{pmatrix} Q_{11} & Q_{12}\\ Q_{21} & Q_{22}\end{pmatrix} \begin{pmatrix} c_{21}^*\\ c_{22}^*\end{pmatrix} d\Gamma
\end{aligned}
\tag{17}
$$

with the coefficients:

$$
\begin{aligned}
Q_0 &= \frac{\omega\gamma\gamma^*\nu}{2(\gamma^2 - \gamma^{*2})},\\
Q_{11} &= Q_{22} = (\gamma - \gamma^*)\left(e^{\frac{d}{2}(\gamma+\gamma^*)} - e^{-\frac{d}{2}(\gamma+\gamma^*)}\right),\\
Q_{12} &= Q_{21} = (\gamma + \gamma^*)\left(e^{-\frac{d}{2}(\gamma+\gamma^*)} - e^{\frac{d}{2}(\gamma+\gamma^*)}\right),
\end{aligned}
\tag{18}
$$

and the total losses by:

$$
\begin{aligned}
P = &\int_\Gamma P_0 \begin{pmatrix} c_{11} & c_{12}\end{pmatrix} \begin{pmatrix} P_{11} & P_{12}\\ P_{21} & P_{22}\end{pmatrix} \begin{pmatrix} c_{11}^*\\ c_{12}^*\end{pmatrix} d\Gamma\\
&+ \int_\Gamma P_0 \begin{pmatrix} c_{21} & c_{22}\end{pmatrix} \begin{pmatrix} P_{11} & P_{12}\\ P_{21} & P_{22}\end{pmatrix} \begin{pmatrix} c_{21}^*\\ c_{22}^*\end{pmatrix} d\Gamma
\end{aligned}
\tag{19}
$$

with the coefficients:

$$P_0 = \frac{\sigma}{2(\gamma^2 - \gamma^{*2})},$$
$$P_{11} = P_{22} = (\gamma - \gamma^*)\left(e^{\frac{d}{2}(\gamma+\gamma^*)} - e^{-\frac{d}{2}(\gamma+\gamma^*)}\right), \tag{20}$$
$$P_{12} = P_{21} = (\gamma + \gamma^*)\left(e^{\frac{d}{2}(\gamma+\gamma^*)} - e^{-\frac{d}{2}(\gamma+\gamma^*)}\right).$$

3.3 C The nonlinear case

For nonlinear materials, no analytic solution of the cell problem (7) exists. The main idea of the effective interface formulation is to find effective parameters γ_{eff} and $\boldsymbol{\nu}_{eff}$ so that the function defined by (8) and (9) gives a good approximation of the nonlinear solution in a meaningful averaged sense. If such parameters are known, the interface formulation (12) can be used as-is in a nonlinear iteration where the effective parameters are updated in each step.

To define suitable effective parameters, we require that the ficticious reactive power given by (15) is exactly reproduced by the effective solution $\boldsymbol{A}_{eff}$ in the cell problem, i.e. for any point on the shield and for given tangential solution components $A_i^{\pm}$ on either side, we require that:

$$\frac{\omega}{2}\int_{-\frac{d}{2}}^{\frac{d}{2}} \nu \widetilde{\boldsymbol{B}} \cdot \widetilde{\boldsymbol{B}}^* d\eta = \frac{\omega}{2}\int_{-\frac{d}{2}}^{\frac{d}{2}} \nu_{eff} \widetilde{\boldsymbol{B}}_{eff} \cdot \widetilde{\boldsymbol{B}}_{eff}^* d\eta. \tag{21}$$

As a first step, we calculate the average total magnetic flux density $\overline{B}$ through the shield by:

$$\overline{B} = \frac{1}{d}\|\boldsymbol{A}^+ - \boldsymbol{A}^-\|. \tag{22}$$

This $\overline{B}$ is then used in the given nonlinear BH-curve to obtain an averaged total magnetic field strength $\overline{H}$ and therefore an averaged magnetic reluctivity $\overline{\nu} = \frac{\overline{H}}{\overline{B}}$. With this, the first effective parameter γ_{eff} is defined as $\gamma_{eff} = \sqrt{i\omega\sigma\overline{\nu}^{-1}}$. Because $\widetilde{\boldsymbol{B}} = \widetilde{\boldsymbol{B}}(\gamma)$, this is sufficient to define the effective solution for the cell problem.

By choosing the second effective parameter $\boldsymbol{\nu}_{eff}$ according to:

$$\nu_{eff} = \frac{\int_{-\frac{d}{2}}^{\frac{d}{2}} \nu \widetilde{\boldsymbol{B}} \cdot \widetilde{\boldsymbol{B}}^* dz}{\int_{-\frac{d}{2}}^{\frac{d}{2}} \widetilde{\boldsymbol{B}}_{eff} \cdot \widetilde{\boldsymbol{B}}_{eff}^* dz}, \tag{23}$$

the relation (21) is fulfilled by definition. This gives rise to the following algorithm.

Let $\boldsymbol{A}_{old}$ be any starting solution. For every integration point on Γ evaluate the tangential components of $\boldsymbol{A}_{old}$ on either side to obtain $A_i^{\pm}$. Use these as boundary conditions for the nonlinear cell problem and solve it to obtain $\widetilde{\mathrm{B}}$. Calculate the effective parameters using (21) and (23). Use these in (13) and (14) to assemble the interface formulation. This yields a solution $\boldsymbol{A}_{new} \in H(\mathrm{curl},\Omega_0)$. Repeat this progress, using $\boldsymbol{A}_{new}$ as the new starting solution, until convergence is achieved.

3.4 D Efficient precomputation

The algorithm given above requires the solution of the nonlinear cell problem for each integration point on Γ and each nonlinear iteration, which, depending on the mesh and the

chosen integration order, might not be feasible due to the increased computation time. To counteract this, the effective parameters are precomputed for a meaningful sample of cell problems and interpolated from these values during the online phase. This is only necessary for $\boldsymbol{\nu}_{eff}$, since γ_{eff} does not require the nonlinear solution and can be computated cheaply from evaluations of $\boldsymbol{A}$.

The cell problem can be fully described by eight real parameters: The real and imaginary parts of A_1^+, A_1^-, A_2^+ and A_2^-. After choosing a maximum value which the total current density is not expected to exceed, one obtains an upper bound A_{max} for the absolute value of each input and a parameter space of $[-A_{max}, A_{max}]^8$, because a-priori all input values have to be assumed to be able to fall anywhere on the complex plane within this limits (see the first line of Figure 2). Naive discretition of this space would lead to an infeasible amount of necessary precomputations, which is why we seek to eleminate as many dimensions as possible using inherent invariants in the problem.

Let L be any linear length-preserving transformation, $\widetilde{\boldsymbol{A}}$ be the solution of (7) for given boundary conditions $\boldsymbol{A}^{\pm}$ and $\boldsymbol{\nu}(\widetilde{\boldsymbol{A}})$ the corresponding nonlinear magnetic reluctivity. For any given BH-curve, $\boldsymbol{\nu}$ depends only on the total magnetic flux, which implies that $\nu = \nu\left(||\widetilde{\mathrm{B}}||\right) = \nu\left(||L\widetilde{\mathrm{B}}||\right)$. Therefore $\widetilde{\boldsymbol{A}}$ and $L\widetilde{\boldsymbol{A}}$ describe the same nonlinear material. Due to the linearity of differential operators, it follows that $L\widetilde{\boldsymbol{A}}$ solves the nonlinear cell problem (7) for the boundary conditions $L\boldsymbol{A}^{\pm}$ and there holds $\gamma_{eff}(\boldsymbol{A}^{\pm}) = \gamma_{eff}(L\boldsymbol{A}^{\pm})$ and $\nu_{eff}(\boldsymbol{A}^{\pm}) = \nu_{eff}(L\boldsymbol{A}^{\pm})$. Therefore one does not lose information about the effective parameters by choosing a normalization of the input based on linear length-preserving transformations.

As a first step, note that every matrix A of the form:

$$A = \begin{pmatrix} a & b \\ -b^* & a^* \end{pmatrix}, \quad \left|\left| \begin{pmatrix} a \\ b \end{pmatrix} \right|\right| = 1 \tag{24}$$

is a linear length-preserving transformation. It can be shown that using the parameters:

$$r = -\frac{A_2^+ + A_2^-}{A_1^+ + A_1^-}, \quad a = r\sqrt{\frac{1}{1 + rr^*}}, \quad b = \frac{a}{r}, \tag{25}$$

there holds $A_1^+ + A_1^- = 0$ for the transformed boundary conditions (see the second row of Figure 2). Because rotations and reflections of a single component are also linear and length-preserving, the first component can be rotated so that $A_1^+ \in \mathbb{R}_0^+$ and the second component so that $A_2^+ + A_2^- \in \mathbb{R}_0^+$. The bottom line of Figure 2 shows this final normalized state. Each set of given boundary condition can be fully described using only the four parameters:

$$A_1^{diff} = |A_1^+ - A_1^-|, \tag{26}$$

$$A_2^{diff} = |A_2^+ - A_2^-|, \tag{27}$$

$$A_2^{av} = \frac{|A_2^+ + A_2^-|}{2}, \tag{28}$$

and the angle α after applying the given transformations, and without loss of information about the effective material.

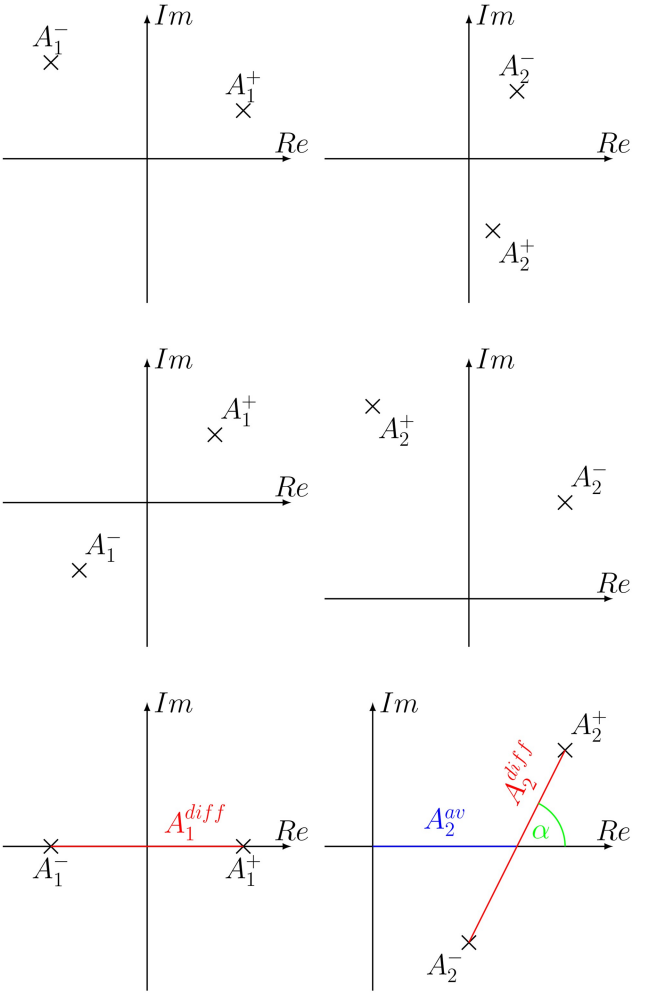

Figure 2. Top: Sample boundary conditions which are distributed arbitrarily on the complex plane. Middle: First normalization step with $A_1^+ + A_1^- = 0$ bottom: Fully normalized conditions and the four remaining degrees of freedom
Source: Authors' own work

Regarding the size of this reduced parameter space, note that only A_2^{av} is directly related to currents. Because it is defined to be non-negative, it suffices to consider $A_2^{av} \in [0, A_{max}]$, i.e. half the size of the original intervals.

Both A_1^{diff} and A_2^{diff} relate to jumps in the magnetic vector potential, i.e. to average magnetic fluxes. Therefore, one has to consider $A_1^{diff}, A_2^{diff} \in [0, B_{max}]$

where B_{max} is the maximum expected flux density. This is usually taken as the saturation state of the material and readily available without requiring any additional knowledge about the problem configuration.

Finally, the angle α between the difference of A_2^+ and A_2^- and the real axis can be assumed to fulfill $\alpha \in \left[0, \frac{\pi}{2}\right]$ by using reflections if $\alpha > \frac{\pi}{2}$.

Therefore, the final parameter space is $[0, A_{max}] \times [0, B_{max}]^2 \times \left[0, \frac{\pi}{2}\right]$ where the last dimension only needs very few sample points for a good discretization.

Note that the cell problem only depends on the material and the shield thickness. Therefore, the same look-up table can be used independently of the problem geometry.

4. Numerical example

Consider an electromagnetic shield over a current loop. To demonstrate that the presented method is able to consider both curved geometries and non-trivial topologies, the shield is chosen as part of a sphere surface and includes a hole. The measures of the shield are shown in Figure 3. The shield is centered above the current loop, with both the center of the loop and the sphere lying on the z-axis. The side view shows the cross section of the geometry at $y = 0$. Behind the shield, an evaluation plane is defined to compare the total magnetic flux for both the reference solution and the effective interface solution. For the top view, note that due to the shield's curvature, the actual side length are larger. The given measures are meant as projections onto the x - y-plane. A depiction of the finite element mesh is included for visualization.

The electric conductivity of the shield is σ = 2MS/m. In air, a negligible fictitious conductivity of σ = 1S/m is chosen for the purpose of regularization. The frequency is f = 50 Hz. The magnetic permeability in air is $\mu = \mu_0$ and in the shield it is given by the nonlinear BH-curve shown in Figure 3. The current loop is not resolved in the mesh.

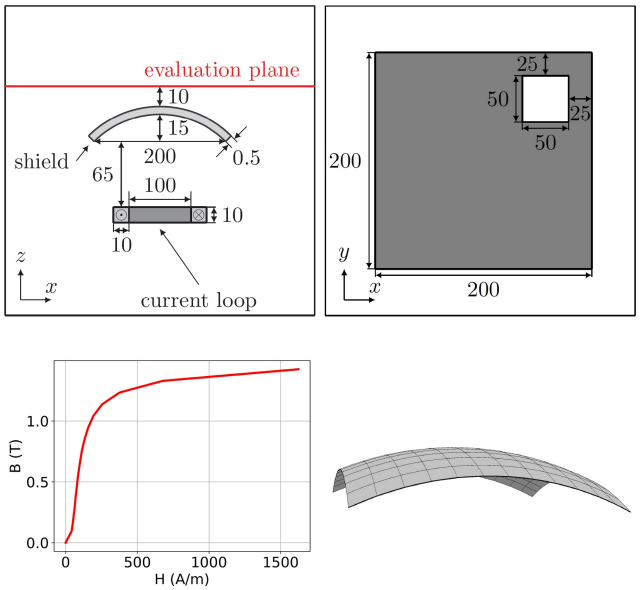

Figure 3. Above: Cross section of the geometry at $y = 0$ (left), top view in the $x - y$-plane (right), all dimensions in mm. Below: the nonlinear BH-curve (left) and the finite element mesh of the shield interface (right)

Source: Authors' own work

The Biot-Savart field of its currents is computed via numerical integration and included as a right hand side as shown in (3). All simulations have been carried out with Netgen/NGSolve (Schöberl, 2025).

As a reference solution, the $\boldsymbol{A}$-formulation is solved for a fully resolved shield. For the effective interface solution, the shield is replaced with a surface in the mesh. The tangential components of $\boldsymbol{A}$ are permitted to jump across the shield surface. The hole is treated like the surrounding air by prescribing tangential continuity for $\boldsymbol{A}$.

As a precomputation step, the cell problem has been solved for $20 \times 20 \times 20 \times 5 = 40,000$ normalized boundary conditions to obtain the respective values of ν_{eff} and store them in a look-up table. For the evaluation of the effective material at a given point, bilinear interpolation of the nearest stored values in four dimensions is used.

In Figure 4 the total magnetic flux density of both the reference solution and the effective interface solution is compared on the plane $y = 0$ and at the evaluation plane defined in Figure 3. Note that while the shield achieves flux densities in the nonlinear range, the scales have been chosen to better illustrate the solution in the whole domain. It can be seen that the effective interface solution yields an excellent approximation of the local fields. Also note the local spike in the magnetic flux density where the shielding quality is reduced due to the presence of the hole.

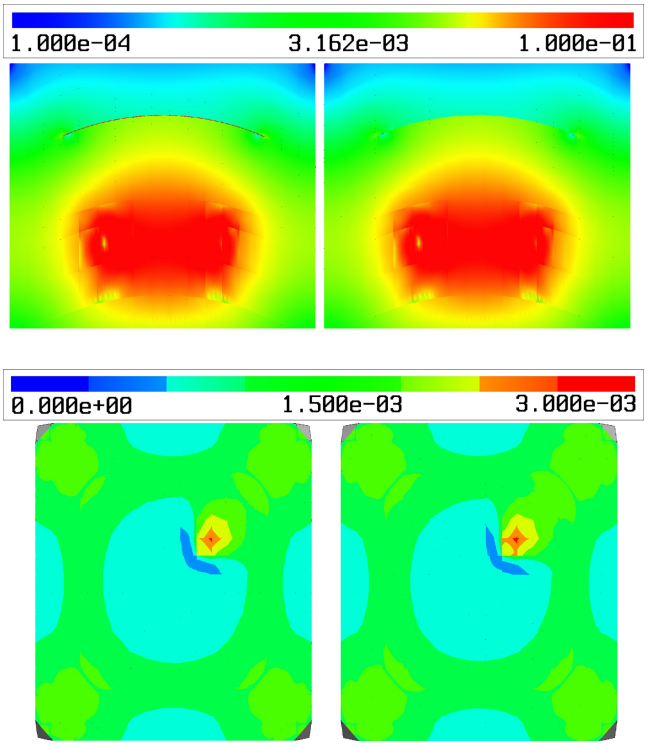

Figure 4. The total magnetic flux at $y = 0$ (above, logarithmic scale) and at the evaluation plane (below) for the reference solution (left) and the effective interface solution (right)
Source: Authors' own work

Table 1. Result data

Q(*ref*) VA	*Q*(*eff*) VA	*Err* %	*P*(*ref*) W	*P*(*eff*) W	*Err* %
0.139	0.132	5.0	0.0445	0.0451	1.3

Note(s): The total reactive power *Q* and total losses *P* inside the shield for the reference solution (ref) and the effective interface solution (eff), and their respective errors (err)
Source(s): Authors' own work

The total reactive power and total eddy current losses inside the shield for the reference solution (according to (15) and (16)) and the effective interface solution (according to (17) and (19)) are given in Table 1. These global properties are also approximated with a high accuracy and a relative error of only a few percent.

5. Conclusion

An interface formulation based on a thin shell model for electromagnetic shielding has been presented. The method is easy to implement since it preserves the problem structure of a linear material where an analytic solution is known. Furthermore, it does not introduce any additional unknowns to deal with the nonlinearity. The solution can be fully described by only the magnetic vector potential in the surrounding air domain.

To efficiently obtain the effective material parameters on the shield interface, a method to reduce the dimensionality of the boundary conditions of the cell problem has been presented, allowing for the construction of a cheap look-up table. The method has been shown to achieve a high accuracy both in a global and a local sense.

References

Biro, O., Bardi, I., Preis, K., Renhart, W. and Richter, K. (1997), "A finite element formulation for eddy current carrying ferromagnetic thin sheets", *IEEE Transactions on Magnetics*, Vol. 33 No. 2, pp. 1173-1178.

Bottauscio, O., Chiampi, M. and Manzin, A. (2006), "Transient analysis of thin layers for the magnetic field shielding", *IEEE Transactions on Magnetics*, Vol. 42 No. 4, pp. 871-874.

de Sousa Alves, B., Sabariego, R.V., Laforest, M. and Sirois, F. (2021), "Hyperbolic basis functions for time-transient analysis of eddy currents in conductive and magnetic thin sheets", *IEEE Transactions on Magnetics*, Vol. 57 No. 11, pp. 1-10.

Del Vecchio, R.M. and Ahuja, R. (2013), "Analytic nonlinear correction to the impedance boundary condition", *IEEE Transactions on Magnetics*, Vol. 49 No. 12, pp. 5687-5691.

Fujita, S. and Igarashi, H. (2019), "Reduction of eddy current loss in rectangular coils using magnetic shield: analysis with homogenization method", *IEEE Transactions on Magnetics*, Vol. 55 No. 6, pp. 1-4.

Geuzaine, C., Dular, P. and Legros, W. (2000), "Dual formulations for the modeling of thin electromagnetic shells using edge elements", *IEEE Transactions on Magnetics*, Vol. 36 No. 4, pp. 799-803.

Hong, Z., Jiang, Q., Pei, R., Campbell, A.M. and Coombs, T.A. (2007), "A numerical method to estimate ac loss in superconducting coated conductors by finite element modelling", *Superconductor Science and Technology*, Vol. 20 No. 4, p. 331, doi: 10.1088/0953-2048/20/4/006.

Igarashi, H., Kost, A. and Honma, T. (1998), "Impedance boundary condition for vector potentials on thin layers and its application to integral equations*", *The European Physical Journal Applied Physics*, Vol. 1 No. 1, pp. 103-109, doi: 10.1051/epjap:1998123.

Koch, S., Trommler, J., De Gersem, H. and Weiland, T. (2009), "Modeling thin conductive sheets using shell elements in magnetoquasistatic field simulations", *IEEE Transactions on Magnetics*, Vol. 45 No. 3, pp. 1292-1295.

Krähenbühl, L. and Muller, D. (1993), "Thin layers in electrical engineering-example of shell models in analysing eddy-currents by boundary and finite element methods", *IEEE Transactions on Magnetics*, Vol. 29 No. 2, pp. 1450-1455.

Liang, F., Venuturumilli, S., Zhang, H., Zhang, M., Kvitkovic, J., Pamidi, S., Wang, Y. and Yuan, W. (2017), "A finite element model for simulating second generation high temperature superconducting coils/stacks with large number of turns", *Journal of Applied Physics*, Vol. 122 No. 4, p. 43903, doi: 10.1063/1.4995802.

Mayergoyz, I. and Bedrosian, G. (1995), "On calculation of 3-d eddy currents in conducting and magnetic shells", *IEEE Transactions on Magnetics*, Vol. 31 No. 3, pp. 1319-1324.

Ortega, J., Lahuerta, O., Carretero, C., Martinez, J. and Acero, J. (2024), "Analytic nonlinear correction to the impedance boundary condition", *COMPEL – The International Journal for Computation and Mathematics in Electrical and Electronic Engineering.*

Rasilo, P., Vesa, J. and Gyselinck, J. (2020), "Electromagnetic modeling of ferrites using shell elements and random grain structures", *IEEE Transactions on Magnetics*, Vol. 56 No. 2, pp. 1-4.

Rodger, D., Atkinson, N. and Leonard, P. (1988), "Transient 3d eddy currents in thin sheet conductors", *IEEE Transactions on Magnetics*, Vol. 24 No. 6, pp. 2691-2693.

Schöberl, J. (2025), "NetGen/NGSolve. [online]", available at: https://ngsolve.org

Schöbinger, M., Tsukerman, I. and Hollaus, K. (2021), "Effective medium transformation: the case of eddy currents in laminated iron cores", *IEEE Transactions on Magnetics*, Vol. 57 No. 11, pp. 1-6.

Taha, H., Henneron, T., Tang, Z., Le Menach, Y., Pace, L. and Ducreux, J.-P. (2023), "Electromagnetic modeling of pcb based on Darwin's model combined with degenerated prism Whitney elements", *IEEE Transactions on Power Electronics*, Vol. 38 No. 1, pp. 678-691.

Corresponding author
Markus Schöbinger can be contacted at: markus.schoebinger@tuwien.ac.at